

ENGINEERING GEOLOGICAL CONDITIONS IN THE CENTRAL AREA OF SHANGHAI
CONDITIONS GÉOTECHNIQUES DANS LA ZONE CENTRALE DE SHANGHAI

Ch. SCHROEDER*, A. DASSARGUES*, X.L. LI**

The engineering geological characteristics (mainly the geotechnical conditions) needed for input in the model have been determined by a compilation, as exhaustive as possible, of existing data, available in several Chinese scientific departments.

This information has been completed by in situ tests and by laboratory tests performed in Shanghai or in Belgium.

Geotechnical formations

The previous studies of the geotechnical conditions in Shanghai have led to the division of the upper seventy meters of the Quaternary overburden into six geotechnical formations, from top to bottom as follows :

1. Superficial layer

The upper part of this first formation is composed of brownish-yellow silts. The lower part consists of mixed silty sand and silts. The superficial layer contains the *phreatic aquifer*.

2. First compressible layer

The top of this formation is between 3 and 20 m depth, its thickness being around 3 to 12 m.

The upper part consists of muddy silts interlayered with silty sands. The lower part consists of muddy clay.

3. Second compressible layer

The top of the formation is at about 20 to 40 m depth, the thickness being in the range 5 to 20 m.

The upper part consists of muddy clay, the middle one of grey silty sand mixed with silty loess.

The lower part contains grey muddy silts interstratified with silty sands, organic material and some gas.

4. Dark Green Stiff Clay (D.G.S.C.)

When this important horizon is present, its thickness reaches a maximum of about 8 m. This layer of high

compactness and high strength is often used as a foundation level for piles.

5. First aquifer

This formation consists of fine yellow sand (quartz) with some opaque constituents. The top is situated at 30-45 m depth, the bottom at about 35-65 m.

6. Third compressible layer

This layer, whose top is situated at about 35-45 m depth with a thickness around 20-35 m, is composed of muddy silts and multilayered silts and fine sands.

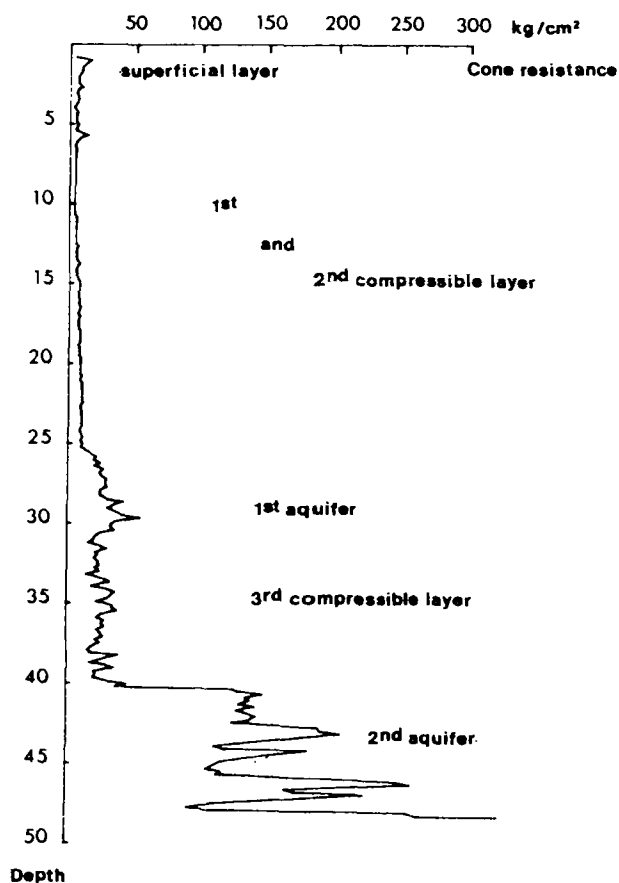


Fig. 1 : A typical example of CPT results.

* Laboratoires de Géologie de l'Ingénieur, d'Hydrogéologie et de Prospection Géophysique, Université de Liège, Liège, Belgique.
** Shanghai Station of Environmental Geology, Shanghai, P.R. China.

7. Second aquifer

The second aquifer consists essentially of fine sands. Its top is situated between 65 and 80 m depth.

In situ tests

The in situ tests consist of some penetration tests (C.P.T.), pressuremeter tests and well logging.

— *Cone penetration tests*

The cone penetration tests have been performed by the Shanghai Geological Center and some additional results come from data by consultants. The main purpose of performing this kind of test was the determination of the foundation level, generally the *Dark Green Stiff Clay layer (D.G.S.C.)*.

Figure 1 shows a typical example of CPT result (diagram of the cone resistance (Q_c), function of the depth).

As a summary, the ranges of the Q_c values are :

- *superficial layer* :
 $700 \leq Q_c \leq 2000$ kPa;
- *first compressible layer and top of the second compressible layer* :
 $200 \leq Q_c \leq 500$ kPa;
- *lower second compressible layer* :
 $450 \leq Q_c \leq 1600$ kPa;

- *D.G.S.C. layer* :
 $1500 \leq Q_c \leq 3500$ kPa;
- *third compressible layer* :
 $2000 \leq Q_c \leq 5000$ kPa;
- *second aquifer* :
 10000 kPa $\leq Q_c$.

— *Pressuremeter tests*

Some pressuremeter tests have been carried out in collaboration with the Belgian team. As results, they give a range of the limit pressure (p_l) from 400 to 1200 kPa and pressuremeter modulus (E_p) from 5 to 18 MPa kg/m^2 for layers between 0 and 25 m depth. These results permit improvement of the laboratory data, but they were too few to allow direct calculations of geotechnical parameters.

— *Well-logging*

The well-loggings, gamma-ray, gamma-gamma and neutron-neutron, have been performed in collaboration with the Chinese team, in eleven boreholes with 70 m to 150 m logged.

They have provided information on clay-content, density and water content which has been used in the correlations and interpretations in order to define more clearly the complex geometry of the different formations.

An example of well-logging is given on Figure 2 where it should be noted that occurrence of gas in the *second*

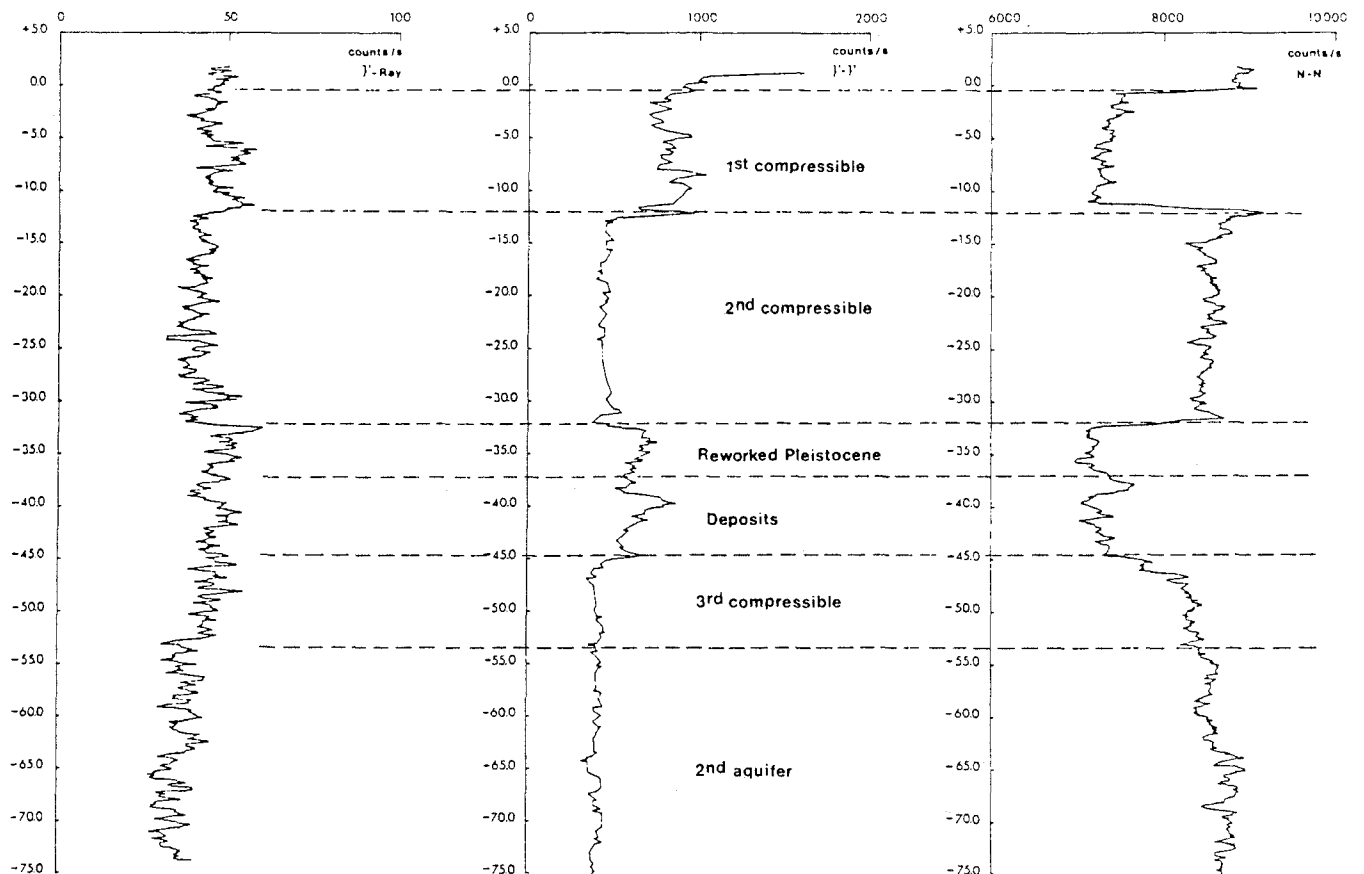


Fig. 2 : γ -ray, γ - γ and neutron well-logging.

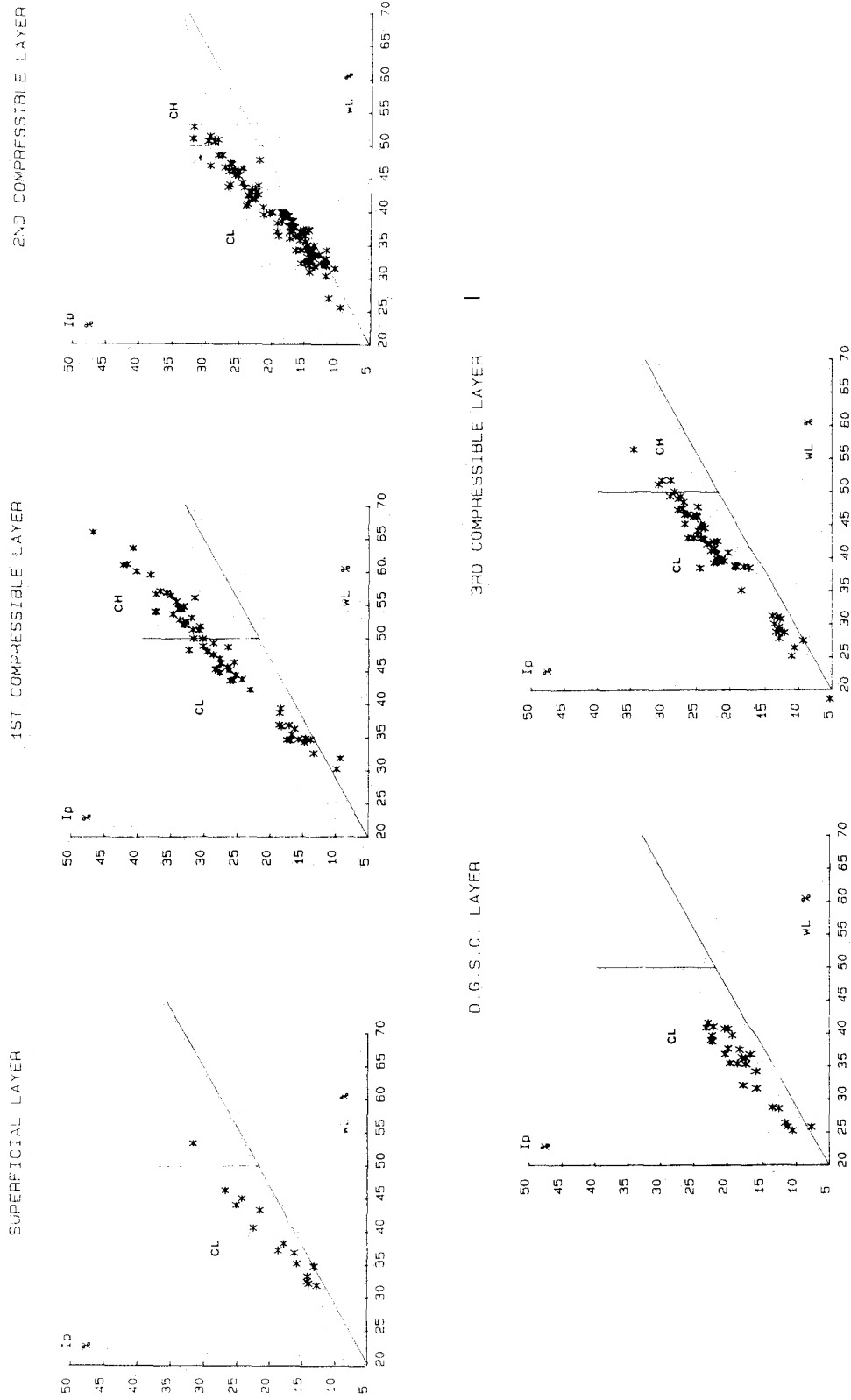


Fig. 3 : Plasticity diagrams.

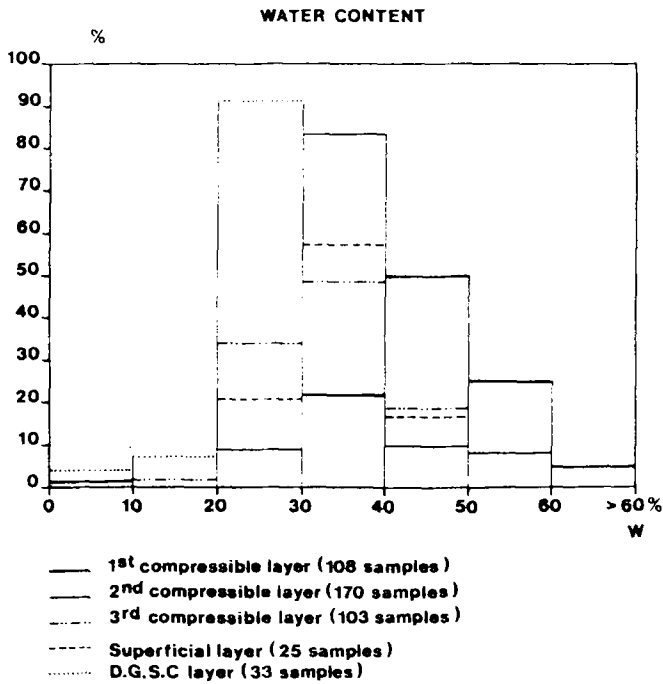


Fig. 4: Histogram of the water content.

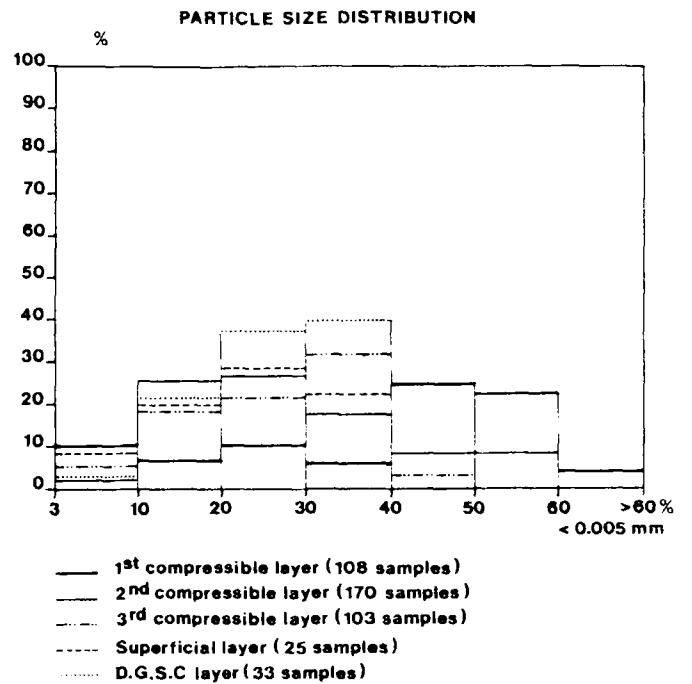


Fig. 5: Histogram of the percentage of particle size lower than 0.005 mm.

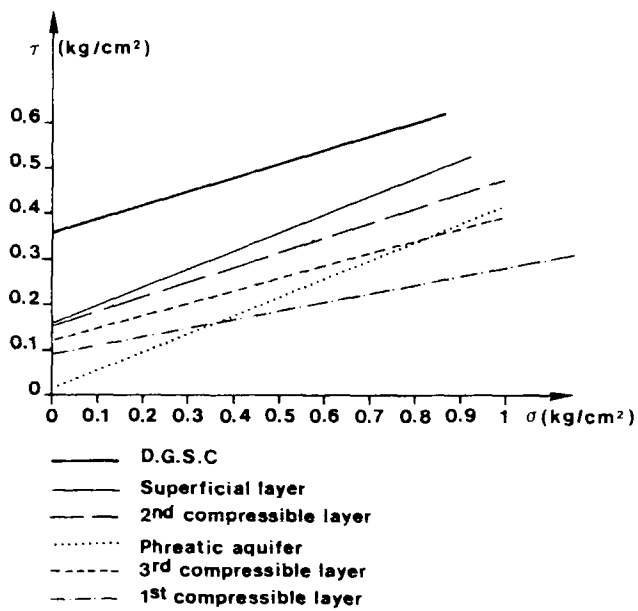


Fig. 6: The Mohr-Coulomb failure envelopes.

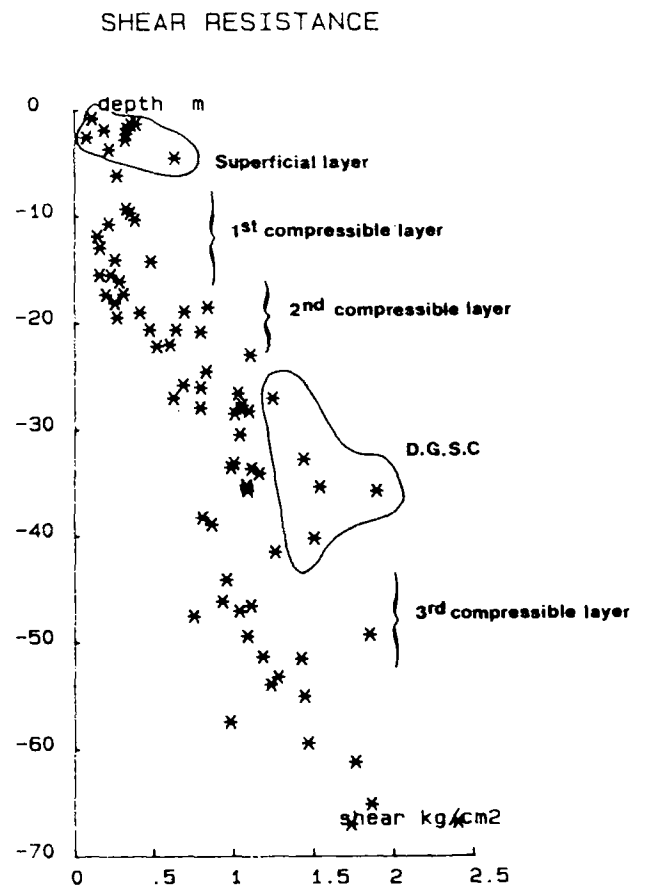


Fig. 7: Diagram of the shear resistance versus depth.

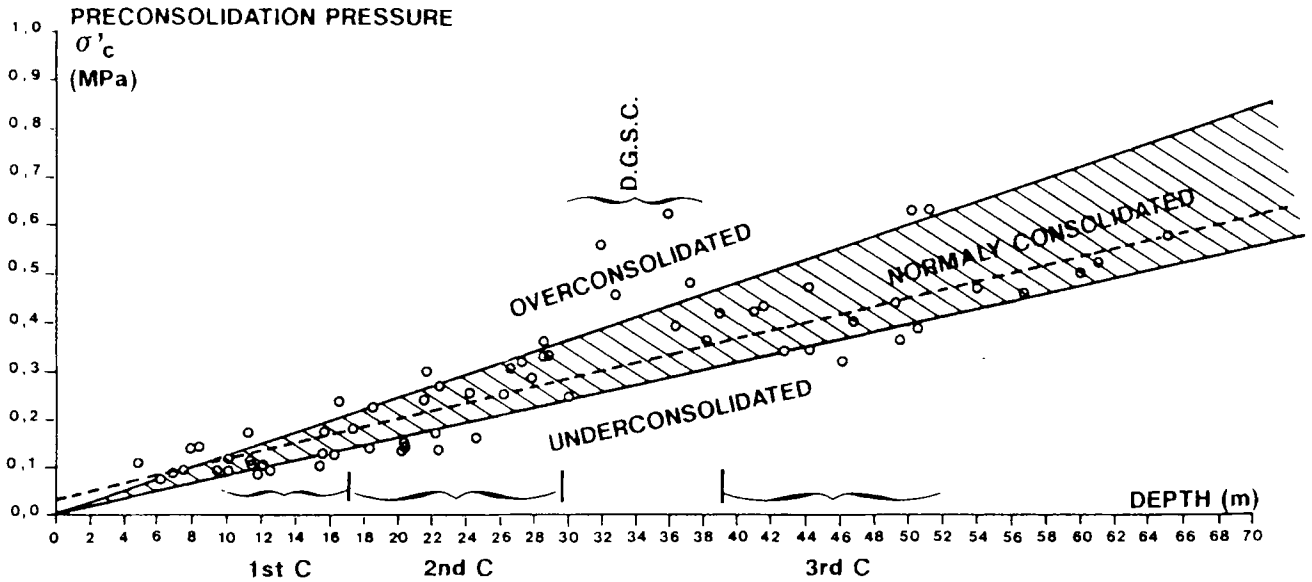


Fig. 8 : Measured preconsolidation pressures versus depth.

compressible layer is particularly evident in the neutron-neutron log.

Laboratory tests

About 450 laboratory tests, mainly "identification" tests have been compiled. In addition, about twenty triaxial, consolidation (oedometer) and high pressure consolidation tests have been carried out in Shanghai and in Belgium. The clay minerals have been investigated by the X-ray method. The results can be summarized as follows :

a. Physical properties

They are deduced from identification tests on disturbed and undisturbed samples with measurement of :

- moisture content, per cent of dry weight;
- Atterberg's limits, liquid w_L , plasticity index I_p ;
- dry unit weight γ_d ;
- percentage of particle size diameter lower than 0.005 mm and 0.002 mm.

From these parameters and assuming the value of the unit weight of solids ($\gamma_s = 2.7 \text{ g/cm}^3 = 25.48 \text{ kN/m}^3$) the following parameters are deduced :

- porosity $n = (\gamma_s - \gamma_d) / \gamma_s$;
- void ratio $e = (\gamma_s - \gamma_d) / \gamma_d$;
- submerged unit weight $\gamma = \gamma_d (1 + w)$.

1) Plasticity characteristics

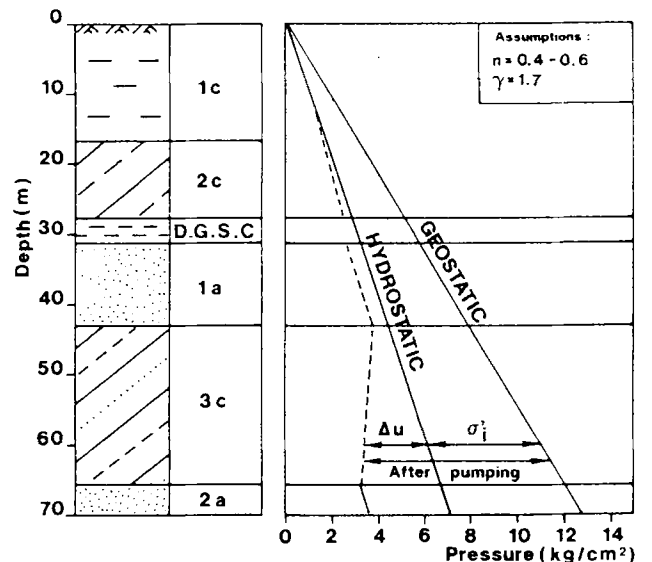
The plasticity diagrams (Fig. 3) are plotted for the different geological units distinguished by the Quaternary analysis.

According to the U.S.C.S. classification the majority of the samples may be qualified CL (CL = Clay of Low

compressibility) but CH (CH = Clay of High compressibility) is also distinguished in the first compressible layer.

2) Particle size distribution and water content

Histograms of the water content (Fig. 4) and of the percentage of particle size lower than 0.005 mm (Fig. 5), illustrate the higher plasticity of the first compressible layer.



- 1c : 1st compressible layer
- 2c : 2nd compressible layer
- 1a : 1st aquifer
- 3c : 3rd compressible layer
- 2a : 2nd aquifer

- Δu : Pore pressure decrease due to pumping
- σ'_i : Initial effective stress

Fig. 9 : Stresses and pore pressure evolutions.

The relations between dry unit weights and moisture contents are nearly the same for each layer proving the assumed non-variability of the grains unit weight.

b. Mechanical properties

1) Strength tests

Consolidated undrained (C.U.) triaxial compression tests have been performed on undisturbed samples. The Mohr-Coulomb failure envelopes are deduced for samples taken from the different layers (Fig. 6) and the shear resistance (by simple shear tests) is plotted versus depth (Fig. 7). The results indicate that :

- the D.G.S.C. layer is stronger and possesses a cohesion and a higher shear resistance;
- the phreatic aquifer (samples were probably disturbed) has no cohesion;
- the first compressible layer (mainly between - 10 and - 20 m) is less resistant.

2) Compressibility

High and low pressure oedometer tests have been performed on undisturbed samples from each clayey layer. The compression index C_c , the consolidation coefficient C_v and the permeability K have been calculated for each loading step. The ranges of C_c values for the different layers are obtained :

- *phreatic aquifer* $0.04 \leq C_c \leq 0.09$
- *first compressible layer* $0.4 \leq C_c \leq 1.2$
- *second compressible layer* $0.3 \leq C_c \leq 1.2$
- *D.G.S.C. layer* $0.2 \leq C_c \leq 0.4$
- *first aquifer* $0.2 \leq C_c \leq 0.3$
- *third compressible layer* $0.3 \leq C_c \leq 0.5$
- *second aquifer* $0.15 \leq C_c \leq 0.2$

The preconsolidation stress has been determined and compared to the actual in situ stress, assuming a bulk density of 1.8 and 2.2 g/cm³. The *first and second compressible layers* are normally consolidated, the *third compressible layer* is slightly overconsolidated and the *D.G.S.C.* is obviously overconsolidated. The slight *overconsolidation of the third compressible layer* may have been induced by the consolidation due to the important pumpings before 1965.

About 60 values of the preconsolidation stress are drawn as function of the depth on Figure 8. The linear correlation is

$$\sigma'_c = 0.31 + 0.084h \quad (h = \text{depth})$$

with a correlation coefficient = 0.94

For the computation of the settlements, the knowledge of the initial void index, e_{ini} , is needed (Dassargues et al., 1989). Now, all the oedometer tests have been carried out during the last 20 years so that no test has been run on "intact" samples. The tested soils have been already consolidated because of the pumpings.

The evolution of the effective stresses from 1920 up to the date of the test is known according to the Ter-

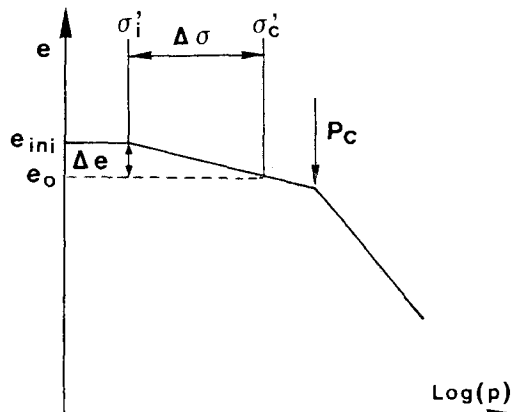
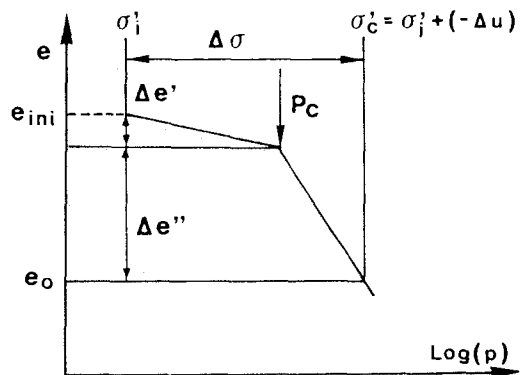
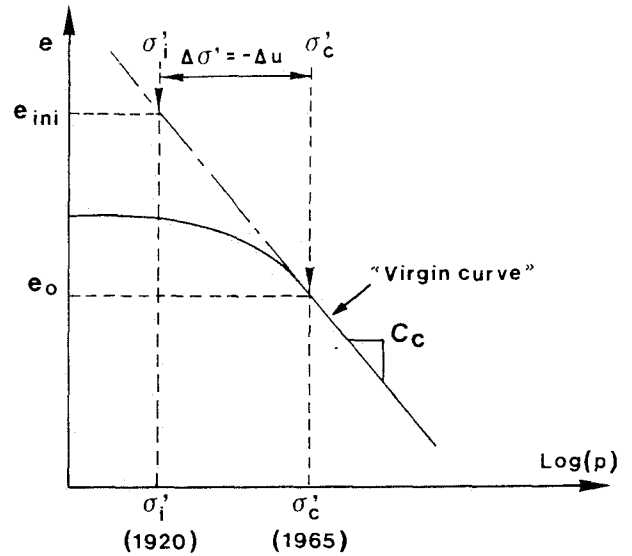


Fig. 10: Determination of e_o .
Normally consolidated soils.

zaghi's principle ($\Delta\sigma' = -\Delta p$, variation of the pressure produced by the pumping, see Figure 9).

The initial void ratio, in 1920, has been calculated from the results of the present tests (Dassargues et al., 1989).

For the calculation of $e_{init} = e_0 + \Delta e$, 2 cases could occur :

— normally consolidated soils (Fig. 10) as *1st, 2nd, 3rd compressible layers and 1st and 2nd aquifer* :

$$\Delta e = C_c \cdot \log [(\sigma'_i + \Delta\sigma')/\sigma'_i]$$

— overconsolidated soils : *D.G.S.C. layer*. Two cases :

• the ground has only an elastic rebound if

$$\Delta\sigma' = -\Delta u \leq (\partial'p - \sigma'_i) \text{ and } \Delta e \text{ is very small (Fig. 11).}$$

• $\Delta\sigma' = -\Delta u > (\sigma'_p - \sigma'_i)$ and (Fig. 12)

$$\Delta e = \Delta e_c + \Delta e''$$

$$= C_s \log (\sigma'_p/\sigma'_i) + C_c \log [(\sigma'_i + \Delta\sigma')/\sigma'_p].$$

c. X-ray analyses

Detailed qualitative and quantitative analysis by X-ray diffraction have been performed on more than 50 samples by the Laboratory of Clay Minerals Geology

of the University of Liege (Prof. J. Thorez). The results have shown that illite and kaolinite are the dominant clay components. Beside them, the complex clay association is such that no clear cut or evolution can be traced. The trends in occurrences of water acceptors and swelling components have been determined. These properties are to be linked to the compressibility of the sediment under drained consolidation.

Conclusion

The geotechnical data gathered by the compilation of existing data and improved by in situ and laboratory tests provide the characteristics of the seven typical layers of the upper 70 m of the Shanghai sub surface.

The average values and the range of the main parameters are synthetized in Table 1.

Reference

DASSARGUES A., SCHROEDER C. and MONJOIE A., 1989 : The hydrogeology and engineering geology of the Shanghai area. L.G.I.H., Report SPPS/891, Unpublished.

Table 1 : Summary of geotechnical properties.

Geotechnical Properties	Surface layers		Phreatic aquifer		1st compressible layer		2nd compressible layer		DGSC		3rd compressible layer		1st aquifer
	Range	av.	Range	av.	Range	av.	Range	av.	Range	av.	Range	av.	Range
Natural water content w %	23-50	35.5		36	30-60	46.5	28-48	34.6	18-27	24.7	20-44	33	+/- 27
Liquidity limit w_L %	30-46	35.2		30		41.6	29-44	36	25-38	32.6	20-48	37	+/- 27
Plasticity index I_p %	10-21	14			7-31	19.3	8-24	15	8-17	14	8-24	16	
Dry unit weight γ_d g/cm ³	1.17-1.55	1.37		1.26	1-1.49	1.19	1.18-1.68	1.36	1.49-1.71	1.61	1.21-1.7	1.37	
Clay content < 2 μ m %						26	7-35	18.2	6-15	16.5	5-25	17.2	
Silt content < 0.05 mm %	10-38	25	0-7		4-68	37.4	5-58	28.7	9-37	27	7-44	27	2-3
Void index e		0.92		1.01	0.6-1.9	1.34	0.67-1.26	0.97	0.58-0.82	0.7	0.6-1.8	0.96	+/- 0.78
Compressibility A_{1-2} 10.MPa ⁻¹	0.016-0.110	0.039		0.027	0.031-0.025	0.097	0.013-0.008	0.037	0.012-0.025	0.018	0.015-0.12	0.041	+/- 0.016
Internal friction angle ϕ degree	7-34	22		22.5	4-27	9.5	10-29	17.9	9-31	15.2	9-24	15.9	
Cohesion c 10 ² kPa	0.02-0.4	0.15		0.01	0.05-0.1	0.086	0.02-0.52	0.15	0.26-0.58	0.36	0.07-0.18	0.12	
Uniformity coefficient C_u					2.5-13	5.36	3.5-20	10.5	12-50	25	2-36	10.7	
Permeability k_v cm/s				2.10 ⁻³	7-8.10 ⁻⁸		7-8.10 ⁻⁷			6.10 ⁻⁸		4.10 ⁻⁷	